Molecular dynamics in perfluoroneicosane. III. Oscillatory and diffusive translational motion

Thomas Albrecht, Raimund Jaeger, Winfried Petry, Ralf Steiner, Gert Strobl, and Bernd Stühn

Citation: The Journal of Chemical Physics **95**, 2817 (1991); doi: 10.1063/1.460933
View online: http://dx.doi.org/10.1063/1.460933
View Table of Contents: http://scitation.aip.org/content/aip/journal/jcp/95/4?ver=pdfcov
Published by the AIP Publishing

Molecular dynamics in perfluoro-*n*-eicosane. III. Oscillatory and diffusive translational motion

Thomas Albrecht, Raimund Jaeger, Winfried Petry,[a] Ralf Steiner, Gert Strobl, and Bernd Stühn[b]

Fakultät für Physik, Universität Freiburg, Hermann-Herder-Strasse 3, D 7800 Freiburg, Germany

(Received 18 January 1991; accepted 1 May 1991)

The translational motion of $C_{20}F_{42}$ helices is investigated using a combination of x-ray scattering and coherent quasielastic and inelastic neutron scattering techniques. In phase I, the helices are ordered with respect to their orientation and the dominating mode of motion is an acoustic phonon. In the high temperature phase *R*, the helices are disordered with respect to their longitudinal position and the angle of rotation around their main axis. Neutron scattering reveals for the longitudinal disorder a wide spectrum of relaxation times (10^{-12}–10^{-9} s). The rotational ordering of the helices leads to increased correlations and a slowing down in the diffusive longitudinal dynamics already above the phase transition.

I. INTRODUCTION

Molecular crystals of the oligomers of macromolecules may be looked at as model systems for their polymeric analog. In many respects, they provide more direct information on structure and dynamics than the polymer because of the availability of partly ordered polycrystalline powders or even single crystals, but still the size of the molecules and the correspondingly large number of degrees of freedom gives rise to complex structural and dynamic properties. The study of such systems as a particular class of molecular crystals is therefore in itself a fascinating subject. Furthermore, one can hope to gain some insight into the even more complicated problem of the polymer.

In this third of a series of papers, we discuss the translational dynamics in perfluoro-*n*-eicosane ($C_{20}F_{42}$), an oligomer of polytetrafluoroethylene. As was shown in the foregoing publications I[1] and II[2], this substance consists of stiff helical molecules which are arranged in layers of hexagonal symmetry. The layers are stacked on top of each other to produce a lattice of rhombohedral symmetry at room temperature. Lowering temperature to $T_t = 200$ K, one arrives at a first order phase transition at which the crystal transforms into monoclinic symmetry. The transition goes along with a loss of mobility and an ordering of the helices with respect to their handedness.

The purpose of the present paper is a characterization of the molecular motions in the high temperature phase (phase "*R* "). We will focus here on longitudinal motions along the helical axis of the molecules and discuss the rotational degrees of freedom in a forthcoming publication. We use two types of experiment to investigate the molecular motion. One is static scattering of x rays or neutrons. The result is a snapshot of correlations between deviations from the average molecule positions. This disorder gives rise to diffuse scattering which is concentrated in certain regions of reciprocal space as a consequence of the helical structure of the molecule. One such region, the "meridian," is located on the c^* axis of reciprocal space at $c^* = 2\pi/\Delta z$, Δz being the monomer distance along the chain. It is the result of the periodic structure of the molecule along its long axis. Consequently, this scattering intensity may be used to monitor the structure and dynamics of single helices, their correlations, and finally intramolecular defects that disturb the underlying periodicity.

The second experiment aims at the explicit time dependence of the correlations. Using quasi and inelastic neutron scattering techniques[3] we measure the dynamic structure factor $S(q,\omega)$ in the regime $1\ \mu\text{eV} \leqslant \hbar\omega \leqslant 6$ meV. This corresponds to correlation times $10^{-9} \leqslant \tau/s \leqslant 10^{-12}$. The scattering vector $\mathbf{q}$ is related to wavelength λ and scattering angle 2θ via $|q| = (4\pi/\lambda)\sin\theta$. It is important to note that carbon and fluorine are both strong coherent scatterers for neutrons. The experiment is therefore sensitive not only to the individual, but also to the correlated motion of helices.

In the following, we will describe briefly the various types of scattering experiments used. We then give an expression for the dynamic structure factor which allows an interpretation of our results in terms of models for the longitudinal translational mobility. We will show that oscillatory and diffusive modes of motion contribute to this mobility and discuss their significance for the phase transition.

II. EXPERIMENTAL

The perfluoro-*n*-eicosane sample was the same as the one used in papers I and II. Polycrystalline cakes or mats were produced following the procedures described in paper II. The crystals were well oriented with their helix (*c*) axes being distributed in a range of $\pm 10°$ around the surface normal. Within the plane of the cake the *a* and *b* axes showed no preferred direction.

For the x-ray scattering experiments, we employed a Siemens D500 powder diffractometer which had been automated to operate under computer control. The system works in reflection geometry. Sample and detector may be rotated separately. It is therefore ideally suited for the investigation of samples with uniaxial texture. The source of radiation was

[a] Institut Laue Langevin, 156X, 38042 Grenoble, France.

[b] To whom correspondence should be addressed.

 0021-9606/91/162817-06$03.00

a copper anode. Together with a graphite secondary monochromator, the wavelength used was $\lambda_{CuK_\alpha} = 1.542$ Å comprising the α_1 and α_2 components.

All neutron scattering experiments were performed at the Institute Laue Langevin, Grenoble, France. For details of the spectrometers used, we refer to Ref. 4. Here we only collect briefly the important set-up parameters used in our experiments.

The quasielastic scattering was measured with the back scattering spectrometer IN13. At a wavelength $\lambda = 2.23$ Å, the multidetector of this instrument covers a range of $1.2 \leqslant q/\text{Å}^{-1} \leqslant 5.5$ and allows us to measure line broadenings as small as 2 and up to more than 100 μeV (see below). A drawback is the relatively low resolution in scattering angle $\Delta(2\theta) \approx 2°$. However, in the scattering geometry used, the relevant detectors are essentially parallel to the surface of the sample. The average over $\Delta(2\theta)$ therefore coincides with the average over the distribution of axes orientations in the sample and the loss of information is negligible.

In the range of meV energy transfer, we used the high resolution three axes spectrometers IN8 and D10. This method allows independent variation of q and ω and we will present scans of energy transfer at constant q. They were performed with the wave vector k_f of the scattered neutron fixed and the data were corrected for the change of the volume of the resolution ellipsoid during the scan according to known procedures.[5] The elastic diffuse scattering was resolved with 0.28 meV half-width at half-maximum (HWHM) on IN8 and 0.08 meV HWHM on D10.

III. STATIC STRUCTURE OF LONGITUDINAL DISORDER

In this section, we consider disorder with respect to the longitudinal position of the helices in the lattice. The molecules oscillate around their equilibrium positions in a collective manner. This type of disorder, caused by phonons, is one contribution to the Debye–Waller factor. It affects the intensities of Bragg reflections and generates diffuse intensity. A second mode of longitudinal motion is of diffusive nature. In phase R, the helices are free to rotate.[2] Furthermore, there exists a rather soft layer between the stacks of helices in the crystal. As a consequence, the molecules may perform a limited diffusional motion in longitudinal direction. The effect of disorder on the static structure factor as measured in an x-ray scattering experiment was quite generally discussed in paper II. Besides an additional contribution to the Debye–Waller factor of the Bragg reflections, a diffuse scattering component develops which is essentially given by the structure factor of a single helix $|F|^2$:

$$S_d(q_z) = \langle|\Delta F|^2\rangle\left[1 + \sum_{n=1}^{\infty}(C_n \cos nq_z c/3)\right]$$
$$= \langle|F|^2\rangle(1 - e^{-\langle u^2\rangle q_z^2})$$
$$\times\left(1 + \sum_{n=1}^{\infty} C_n \cos n\frac{q_z c}{3}\right) \quad (1)$$

with

$$\langle|\Delta F|^2\rangle = \langle|F|^2\rangle - |\langle F\rangle|^2.$$

$\langle u^2\rangle$ is the mean-square longitudinal displacement of a $C_{20}F_{42}$ molecule.

Equation (1) includes correlations to all neighbors in the distance $nc/3$ with $c \approx 85$ Å being the lattice parameter. However, in the following we will restrict equation 1 to $n \leqslant 2$.

The significance of the correlation coefficient c_n is

$$C_n = \frac{\langle \Delta F_i \Delta F_{i+n}\rangle_i}{\langle|\Delta F_i|^2\rangle_i}. \quad (2)$$

$\langle|F|^2\rangle$ may of course be computed without any approximation. For a qualitative discussion, however, the expression given in I may be used. We thus neglect end groups and restrict our attention to q values on the q_z axis to obtain

$$|F|^2 = (f_C + 2f_F)^2 \sum_{l,l'=0}^{19} e^{i(l-l')\Delta z q_z}. \quad (3)$$

Here f_C and f_F denote the atomic form factors of carbon and fluorine, respectively. For the case of neutron scattering, they are replaced by the corresponding coherent scattering lengths.

It is immediately clear from Eq. (3) that there will be a maximum of diffuse intensity at $q_z = 2\pi/\Delta z$. The monomer distance Δz was determined in I as $\Delta z = 1.30$ Å. Figure 1 shows an x-ray diffraction pattern obtained from the cake sample described in Sec. III. The data clearly show two Bragg reflections (0,0,63) and (0,0,66). The observed splitting of the peaks is caused by the $K_{\alpha 1}$ and $K_{\alpha 2}$ components of the x-ray spectrum. In addition to the peaks, the profile contains a strong diffuse scattering contribution.

The lines drawn in Fig. 1 correspond to a decomposition of the profile according to Eq. (1). The distribution of c axes in the sample as well as the aperture μ of the x-ray beam were explicitly taken into account in a Lorentz factor[6]

$$L = \frac{\text{erf}(\sin\mu/\sqrt{2}\sigma\sin\theta)}{\sin\theta} \quad (4)$$

with σ being the Gaussian width of the Z axis distribution and 2θ the scattering angle. Erf is the error function. The α_1–α_2 splitting as well as the shape of the peak profile were determined separately and used here as fixed parameters. A least-squares fit demonstrates clearly the nonvanishing con-

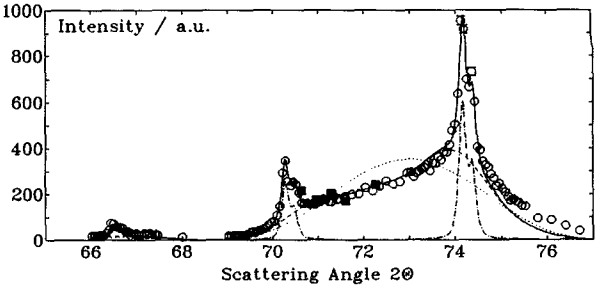

FIG. 1. X-ray scattering profile of $C_{20}F_{42}$ in q_z direction at $T = 219$ K (phase R) (open symbols). The lines drawn are a decomposition of the profile into Bragg and diffuse scattering (see the text). The dotted line corresponds to the single helix structure factor [Eq. (3)]. The broken line shows its modification by the correlation term [Eq. (1)]. The full symbols are the integrated intensities from the inelastic neutron scattering (see the text).

tribution of the correlation component described by the parameter C_1 in Eqs. (1) and (2).

The temperature dependence of the correlation factors C_1 and C_2 is displayed in Fig. 2 for $T \geqslant T_t$. The next neighbor correlations in the diffuse scattering component decrease continuously with increasing temperature and become negligible at room temperature. The remaining diffuse scattering is well described by the superposition of Bragg peaks plus a single helix structure factor, although the helix then contains defects ("reversals"). Their main effect, however, is a loss of handedness as seen in the "torus regime" of the diffuse scattering.[2] The periodicity of the electron density with the monomer distance along the helix axis appears not to be affected.

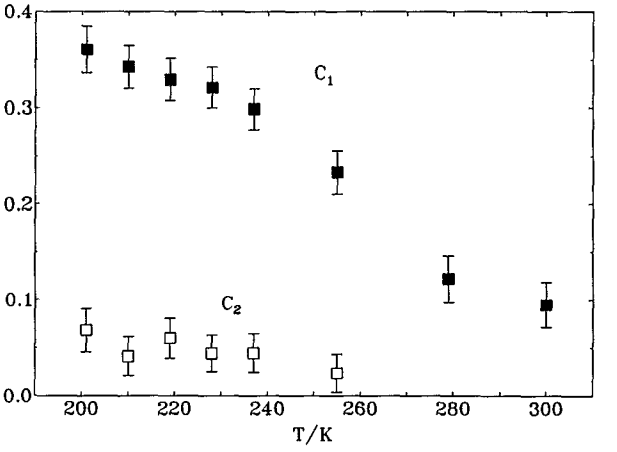

FIG. 2. Temperature dependence of the correlation coefficients C_1 and C_2 [cf. Eq. (2)].

IV. LONGITUDINAL DYNAMICS

We now turn to a discussion of the time dependence of the disorder described above. Depending on the time scale of an experiment, one will expect to be sensitive to oscillations of the helices around their equilibrium position or to their diffusion within the soft layer of end groups between stacks. The thickness of this layer is 2 Å. In the following, we will start with a discussion of the short time limit of 10^{-12} s and follow the dynamics up to correlation times of 10^{-9} s.

For the investigation of the short time scale, we employ the typical three axes inelastic neutron spectrometry and obtain spectra as displayed in Fig. 3. The spectra consist of two inelastic lines at energy transfers $\hbar\omega \simeq 1$ meV which corresponds to oscillations of frequency $\omega \simeq 1.5 \times 10^{12}\ \mathrm{s}^{-1}$. The lines are broadened strongly with respect to the instrumental resolution. In addition to this inelastic contribution, one observes a central component which again is of finite width. Spectra were taken between the layer reflections 64 and 64.5 which correspond to one half of the Brillouin zone in a lattice cell comprising one layer of helices in c direction.

As there are obviously oscillatory as well as diffusive parts present in the spectrum, we use the following scattering law:

$$\frac{S(q,\omega)}{|F|^2} = \tilde{A}_P \frac{\omega}{1-\exp(-\hbar\omega/kT)} \times \frac{\gamma_P(q)}{[\omega^2-\omega_0^2(q)]^2+[\gamma_P(q)\omega]^2} + A_L \frac{\Gamma_L/2\pi}{\omega^2+(\Gamma_L/2)^2} + A_\delta \delta(\omega). \quad (5)$$

Equation (5) represents the superposition of a damped phonon of intensity $\propto \tilde{A}_p$,[5] a quasielastic part given as a Lorentzian of full width at half-maximum Γ_L and intensity A_L and an unresolved central line which is described by a δ-function and intensity A_δ. The phonon at frequency $\omega_0(q)$ has a damping constant γ_p which is inversely proportional to the phonon lifetime. The functional form used here is the response function of the damped harmonic oscillator.[5,7] This renders the constant $\tilde{A}_p$ dependent on the mass of the model oscillator.

The Lorentzian part results from a relaxation of structure factor fluctuations due to diffusive motion.[3] In the time domain, it transforms into a relaxational component of the

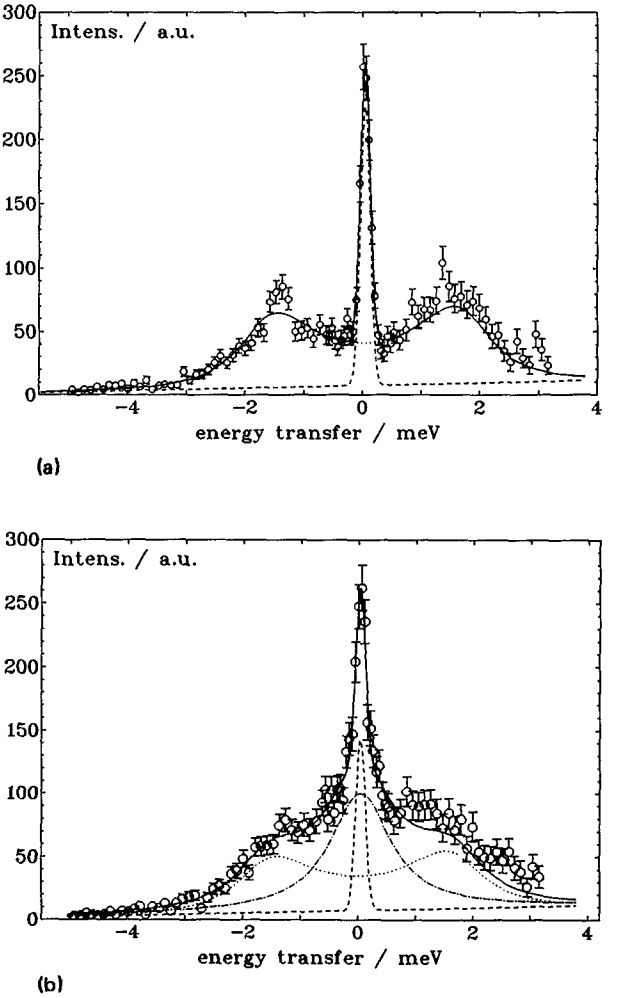

FIG. 3. The inelastic structure factor of $C_{20}F_{42}$ (a) below and (b) above the phase transition at $l = 64.5$. The drawn line is the sum of the phonon (dotted), the quasielastic (dotted–dashed), and an unresolved central component (dashed).

intermediate scattering law $\tilde{S}_L(q,t) \propto \exp(-t/\tau_L)$ with $\tau_L = 2/\Gamma_L$.

An expression similar to Eq. (5) is used in the discussion of soft mode and central peak phenomena[5] and for a description of the combined oscillatory and diffusive motion of particles in liquids.[7] In both cases, one assumes the corresponding time scales to be well separated, i.e., $\omega_0(q) \gg \Gamma_L$.

Finally Eq. (5) is convoluted with the energy resolution of the instrument which was determined in a separate measurement using the incoherent elastic scattering from vanadium. This implies an approximation for the phonon linewidth because the experimental width of an undamped phonon is not exactly that of vanadium. In a least-squares procedure, this model is fitted to the energy loss side of the data. The agreement between the model and our data is very good as may be seen in Figs. 3(a) and 3(b).

The position of the inelastic peak shows clearly dispersion and within the experimental accuracy it is well described as a longitudinal acoustic phonon. The results are shown in detail in Fig. 4. The points correspond to the peak positions as obtained from the individual spectra whereas the lines are the dispersion curve of an acoustic phonon with only next neighbor interaction. Using this assumption in a combined fit of all spectra, one arrives at a velocity of sound of $v = 4.0\ (\pm 2) \times 10^3$ m/s at $T = 180$ K. This value agrees well with recently published data from a Brillouin scattering experiment.[8] There the elastic modulus was related to the moduli of the layers of helices and the interlayer, respectively.

No drastic change was found for the phonon frequencies below and above the phase transition at T_t (see Fig. 4). The same applies to the phonon widths. As is seen in Fig. 5, there is no change with temperature. However, the phonon width increases in approaching the zone boundary which is typical for a finite phonon lifetime caused by anharmonic contributions to the intermolecular potential.[7] The wave vector dependence of the phonon intensity is found to be well described by the single helix structure factor $|F|^2$. Together with the absence of any discontinuity in the lattice parameter c at the phase transition,[2] we are led to the conclusion that the short time lattice dynamics is not involved in the phase transition.

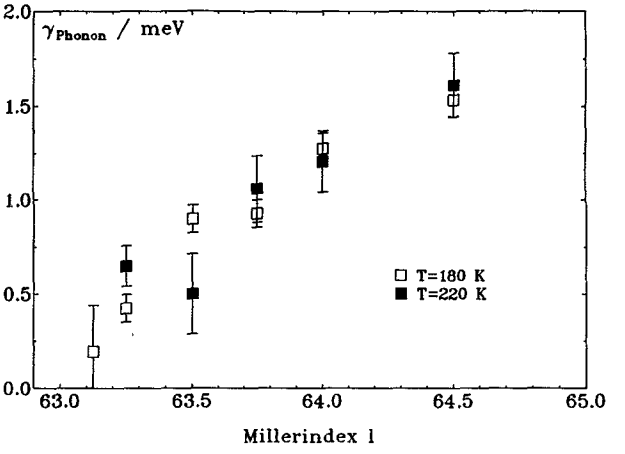

FIG. 5. Phonon width for $T = 180$ and 220 K.

The coherent inelastic neutron scattering experiment decomposes the diffuse scattering observed in the x-ray profiles into a phonon and a central line component. One should therefore recover the wave vector dependence of the x-ray scattering intensity in the integral intensities of the inelastic neutron scattering experiment. This comparison is included in Fig. 1. A common scale factor has been applied to the neutron intensities. In particular, we find the intensity of the unresolved central component on D10 well described by the structure factor given in Eq. (1). Figure 6 displays the remaining q dependence after dividing by the trivial single helix structure factor $|F|^2$. The dotted lines are obtained using Eq. (1) with $n = 2$. The parameters C_1 and C_2 vary from 0.65 and 0.27 below T_t to 0.57 and 0.10 above T_t, respectively. The central line intensity therefore is modulated with the correlations of helix displacement in adjacent layers. We will come back to this point in the discussion of the high resolution experiment on this part of the structure factor.

A striking effect of the phase transition is the sudden

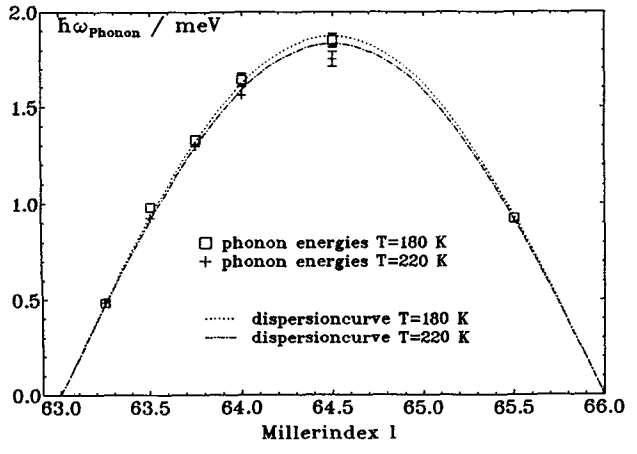

FIG. 4. Phonon peak positions and dispersion curves in phases *I* and *R*.

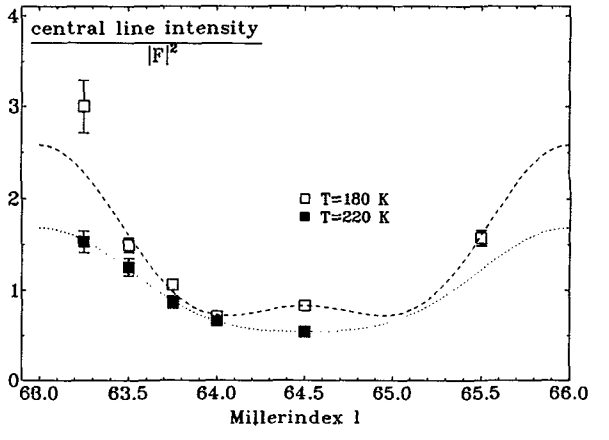

FIG. 6. Integral intensity of the unresolved central line component in the D10 spectra divided by the single helix structure factor. The lines are a fit using Eq. (1).

appearance of the central Lorentz line A_L. At $T = 220$ K, it is clearly present in the spectra at all q values. Its width is

$$\hbar\Gamma_L = 1.26 \text{ meV}$$

independent of wave vector which corresponds to a relaxation time $\tau_L = 6.6 \times 10^{-12}$ s.

The full dynamics of the central line, however, is obviously not completely described by one Lorentzian. Even at $T = 220$ K, there remains about 15% of the central line intensity which is not resolved with the three axes instruments IN8 and D10. For an investigation of this part of the spectrum, we therefore turn to the high resolution backscattering instrument IN13. A typical spectrum obtained at $q_z = 4.82$ Å^{-1} is shown in Fig. 7. the data are corrected for scattering from the cryostat and the sample container. The measured line is broadened clearly with respect to the instrumental resolution. It cannot be fitted with only one Lorentzian convoluted with the instrumental resolution. Using two Lorentzians and a flat background, one arrives at a satisfactory description of the measured spectrum. The flat background is clearly the broad line observed in the wider energy window of the three axes experiment. Its sudden appearance at the phase transition is confirmed in this measurement. The two Lorentzian lines display a further wide interval in time or frequency present in the dynamics. One Lorentzian is of the width 113 μeV independent of temperature. The second line is strongly T dependent (see Fig. 8) and of width $2 \leqslant \gamma_L/\text{meV} \leqslant 5$.

The full spectrum of relaxation times at $T = 220$ K ranges from 6.6×10^{-12} to 10^{-9} s. It is modeled as the sum of three Lorentzian lines in order to arrive at a quantitative means of data evaluation. The preceding paragraphs have demonstrated the interrelation between the phase transition at T_t and the diffusive longitudinal dynamics of the helices. In approaching T_t from above, the spectrum of relaxation times is shifted to longer times. The intensity of the central line increases indicating an enhancement of collectivity in the longitudinal translational motion of the molecules.

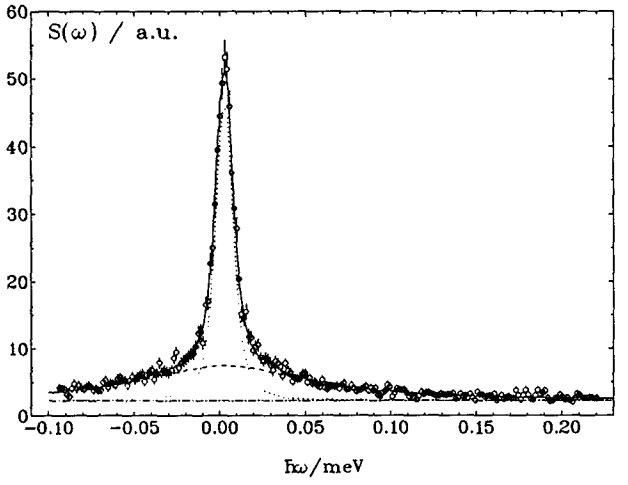

FIG. 7. High resolution spectrum of $C_{20}F_{42}$ at $T = 220$ K and $q = 4.82$ Å^{-1}. The lines drawn are a fit of two Lorentzians and a flat background (see the text).

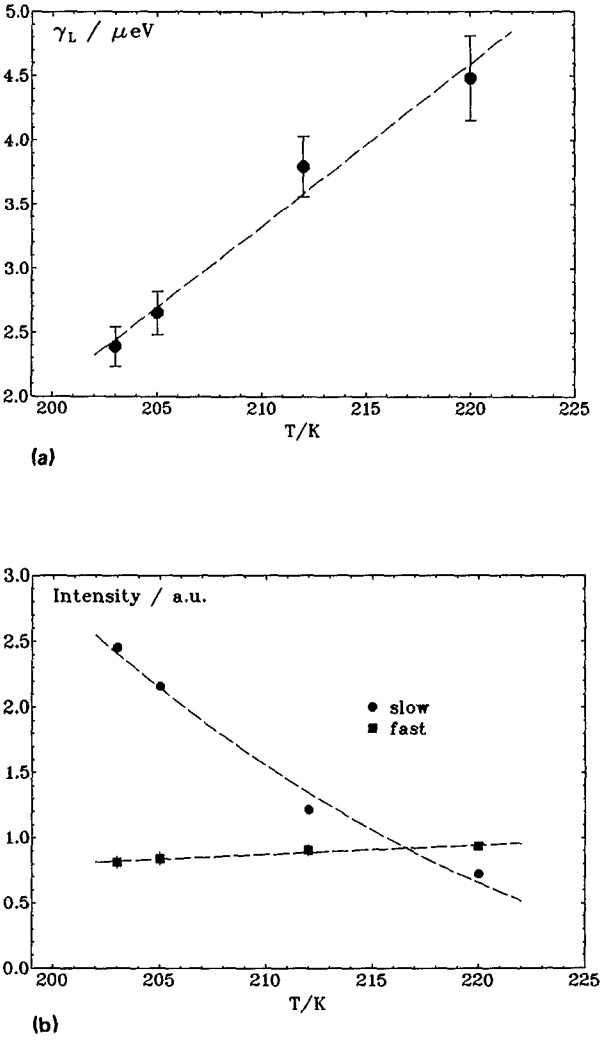

FIG. 8. (a) FWHM and (b) intensity of the Lorentzian lines observed in the back scattering experiment. The lines are guide lines for the eye.

V. CONCLUSION

The investigation of the full dynamic structure factor of $C_{20}F_{42}$ showed that the meridian intensity contained contributions from oscillatory as well as diffusive components. The oscillatory part turned out to be a longitudinal phonon with rather short lifetime. Its dispersion is well described assuming only next neighbor interaction. The interaction forces between helices in adjacent layers in the $C_{20}F_{42}$ crystal are weak compared to the intrahelical forces.

The interface between layers is composed of the fluorine end groups of the molecule. They form a layer of weakly interacting spheres. The helices oscillate according to this small restoring force and explore a wide range of the interaction potential. The contribution of an harmonic terms is correspondingly large and gives rise to short phonon lifetimes. There is only a minor change in the oscillatory motion between phases R and I. Obviously the onset of the rotational motion of the helices at the transition does not affect the longitudinal oscillations.

The diffusive component could be quantitatively analyzed assuming displacements of the helices from their equi-

librium positions in c direction. The displacement in successive stacks appears to be partly correlated. The correlation decays with increasing temperature above the phase transition. These correlations show up in the static x-ray profiles as well as the quasielastic part of the dynamic structure factor.

The diffusive longitudinal motion appears to be dependent on the state of rotational order. As a consequence of the helical structure of the $C_{20}F_{42}$ molecule, rotational order also implies a fixing of its longitudinal position. The molecule is locked in its surrounding just like a screw in this thread. Below T_t (in the rotationally ordered phase I), one finds diffuse scattering which is static on the energy scale of the backscattering instrument. Its relaxation times must be longer than 10^{-8} s. The onset of rotational disorder at the phase transition goes along with a sudden increase in translational mobility.

The relaxation time spectrum in the intermediate range ($10^{-11} \leqslant \tau/s \leqslant 10^{-10}$) appears to be related to the individual motion of the helices. Below room temperature, one finds an additional contribution of a slower component ($\tau \approx 10^{-9}$ s). Together with the results from the static scattering, we interpret this as a correlated longitudinal motion of successive helices. It can be understood as a consequence of the buildup of a short-range rotational ordering already in phase R.

A further remarkable feature of the relaxation time spectrum is the existence of a fast component ($\tau \sim 10^{-12}$ s) immediately above T_t. The underlying mode of motion is not affected by the short-range rotational ordering which is clearly visible in the slow relaxation times. A possible mechanism would be a screw type motion which is not hindered by rotational order and enables fast longitudinal fluctuations. A prerequisite, however, is sufficient disorder in the interface to enable longitudinal molecular motion. This picture is indeed supported by measurements of the rotational diffusion which will be reported in a forthcoming paper. The relaxation times found in these experiments are the same as the fast longitudinal mode.

ACKNOWLEDGMENT

Support of this work by the Ministerium für Forschung und Technologie is gratefully acknowledged.

[1] H. Schwickert, M. Kimmig, and G. Strobl, J. Chem. Phys. **95**, 2800 (1991).
[2] T. Albrecht, H. Elben, R. Jaeger, M. Kimmig, C. Ritter, H. Schwickert, R. Steiner, G. Strobl, and B. Stühn, J. Chem. Phys. **95**, 2807 (1991).
[3] M. Bée, *Quasielastic Neutron Scattering* (Adam Hilger, Bristol, 1988).
[4] H. Blank and B. Maier, *Guide to Neutron Research Facilities At The ILL* (Institut Laue Langevin, Grenoble, France, 1988).
[5] B. Dorner, *Coherent Inelastic Neutron Scattering in Lattice Dynamics* (Springer, New York, 1982).
[6] R. Jaeger, thesis, Universität Freiburg, 1990.
[7] S. W. Lovesey, *Theory of Neutron Scattering from Condensed Matter* (Clarendon, Oxford, 1984), Vol. 1.
[8] A. Marx, J. K. Krüger, and H. Unruh, Phys. B, Condensed Matter **75**, 101 (1989).